Intermittence of transient slow slip in the Mexican subduction zone

Zaccaria El Yousfi, Mathilde Radiguet, Baptiste Rousset, Allen Husker, Ekaterina Kazachkina, Vladimir Kostoglodov

Intermittence of transient slow slip in the Mexican subduction zone

Zaccaria El Yousfi[a], Mathilde Radiguet[a], Baptiste Rousset[b], Allen Husker[c], Ekaterina Kazachkina[d], Vladimir Kostoglodov[d]

[a]*Univ. Grenoble Alpes, Univ. Savoie Mont Blanc, CNRS, IRD, Univ. Gustave Eiffel, ISTerre, , Grenoble, 38000, France*
[b]*Institut Terre et Environnement de Strasbourg, Universite de Strasbourg (UMR 7063), 5 Rue Rene Descartes, Strasbourg, 67000, France*
[c]*Seismological Laboratory, California Institute of Technology, Pasadena, 91125, California, USA*
[d]*Instituto de Geofisica, Universidad Nacional Autonoma de Mexico, Circuito de la, Investigacion Cientifica s/n, C.U., Coyoacan, 04150, CDMX, Mexico*

Abstract

In the Mexican subduction zone, slow slip events of various duration, from a few days to several months have previously been identified in the regions of Guerrero and Oaxaca. They occur along with microseismicity: low-frequency earthquakes and tectonic tremors. In this study, we analyzed a 10-year long tremor catalog covering multiple SSE cycles, to identify periods of high tremor activity. We then used the temporal information of these tremor bursts to decompose GNSS time series. Surface velocities estimated for tremor and non-tremor periods are then inverted to locate slip rates on the plate interface. Combining the detected microseismicity information and GNSS time series, we show that large slow slip events are made of clusters of short-lasting slip events occurring at tremor times and located updip of the tremor area. This analysis also allowed us to unveil low amplitude transients in between large slow slip events, that last 8 – 9 days, occurring at tremor times and locations, in both Guerrero and Oaxaca regions. Finally, we show that the plate locking amplitude in between short and large slow slip events increases by a factor up to 0.5 at the location of tremors.

Keywords: Mexican Subduction Zone, Aseismic Slip, Transient Slow Slip, GNSS, Tectonic Tremor
PACS: 0000, 1111
2000 MSC: 0000, 1111

1. Introduction

Slow slip events (SSEs) are an important component of the seismic cycle in subduction zones, as they release a significant portion of the tectonic stresses accumulated over time. SSEs have been observed in various subduction zones (e.g. in Japan (Hirose et al., 1999), Cascadia (Dragert, 2001), Mexico (Kostoglodov, 2003), and Alaska (Fu and Freymueller, 2013)). They occur mostly downdip from seismogenic zones of young and warm subduction interfaces (Manea et al., 2017), at the transition between the locked and fully creeping zones. Transient slow slip on the plate interface occurs with a wide range of total slip (from a few millimeters to several centimeters), magnitudes (M_w 5 to M_w 7.5), and durations (from a few days to several years) (e.g. Beroza and Ide, 2011). Recent studies show that slow slip is also intermittent, as large-scale SSEs can be decomposed into several smaller slip events clustered in time (Frank et al., 2018; Rousset et al., 2019b). Although SSEs are aseismic and detected geodetically, they are usually accompanied by tectonic tremors (TTs) (Obara, 2002), which are emergent seismic signals of low amplitude and long duration, that are considered to be clusters of low frequency earthquakes (LFEs) (Beroza and Ide, 2011). These seismic markers of slow slip provide valuable information on the temporal characteristics of slow slip processes (Frank et al., 2015a, 2018; Villafuerte and Cruz-Atienza, 2017).

The ability to detect geodetically slow slip signals of small amplitude is limited by the high frequency noise in GNSS time series. The signal to noise ratio of small transients is generally too small for them to be detected

Postprint accepted to Earth and Planetary Science Letters on July 29, 2023. https://doi.org/10.1016/j.epsl.2023.118340

only by GNSS, as they usually last a few days, and generate less than a few millimeters of surface displacement. Several studies proposed combining seismic and geodetic data to isolate small crustal displacements in GNSS time series (Frank et al., 2015b; Frank, 2016; Rousset et al., 2019a; Fujita et al., 2019; Bartlow, 2020), to characterize the short-term dynamics of large-SSEs (L-SSE) (Frank et al., 2018; Rousset et al., 2019b), and test for the existence of smaller-scale transients (Frank et al., 2015b).

In this study, we analyze geodetic time series and seismic tremor catalogs recorded simultaneously in southern Mexico. This combined analysis is performed for the first time using a 10-year long data set, which contains several slow slip event cycles. We aim to investigate the short-term dynamics of transient slip by decomposing GNSS time series using the temporal information of tremor bursts, both during large, previously identified L-SSEs and also in between these.

We study the Guerrero and Oaxaca regions of the Mexican subduction zone (Fig. 1), where the Cocos plate subducts beneath the North America plate with convergence rates increasing from the northwest (62 mm/yr) to the southeast (75 mm/yr) along the middle-America trench. The shape of the subducted slab shows a wide and quasi-horizontal plate interface at $\sim 40 - 45$ km depths, under the states of Guerrero and Oaxaca. Updip on this quasi-flat part of the slab, L-SSEs with equivalent magnitudes M_w 7 − 7.5 and recurrence intervals $\sim$ 4 years occur in Guerrero (Kostoglodov, 2003; Radiguet et al., 2012, 2016; Cruz-Atienza et al., 2021). In Oaxaca, L-SSEs have smaller magnitudes (from M_w 6.5 to M_w 7) and recurrence intervals of $\sim$ 1.5 years (Graham et al., 2016; Cruz-Atienza et al., 2021). In Guerrero, updip from the L-SSEs zone ($<$ 15 km deep), shallow offshore tremor clusters were unveiled (Plata-Martinez et al., 2021), with recurrences of 1 to 3 months. However, most tremors have been identified downdip from the L-SSEs zone, in the flattest part of the slab ($\sim$ 38 to 45 km deep). There, TTs (Payero et al., 2008; Brudzinski et al., 2010; Husker et al., 2012; Cruz-Atienza et al., 2015; Maury et al., 2018) and LFEs (Frank and Shapiro, 2014; Frank et al., 2014) have been detected and localized. Two zones are distinguished on the plate interface in Guerrero: the sweet spot (cluster of the Guerrero tremor zone at depths $>$ 41 km in Fig. 1) where TTs and LFEs occur persistently, and updip, the transient zone (cluster of the Guerrero tremor zone at depths $<$ 41 km in Fig. 1), where the activity of TTs and LFEs is episodic (Husker et al., 2012; Frank et al., 2015a). TT and LFE bursts in the transient zone are correlated in time with the geodetically detected L-SSEs (Frank et al., 2018; Husker et al., 2019). In Oaxaca, TTs occur persistently in the western end of the region at 41 − 50 km depths (Brudzinski et al., 2010; Maury et al., 2018). The TT activity is lower in central Oaxaca. In Guerrero, bursts of LFE activity, with an average duration of 7 − 8 $days$ and an average recurrence time of 3 months have also been detected during before and after the L-SSE of 2006 (Frank et al., 2015b; Villafuerte and Cruz-Atienza, 2017). When combined with tremor/LFE activity, geodetic data showed the existence of short-SSEs (S-SSEs) during the period 2005 - 2007 (Frank et al., 2015b; Villafuerte and Cruz-Atienza, 2017), associated with average surface displacements of 1 − 2 mm and average magnitudes of M_w 6.4 (Frank et al., 2015b). S-SSEs were also detected independently from 2005 to 2012 using a geodetic-matched filter approach (Rousset et al., 2017), with average recurrence intervals of 40 $days$, and durations ranging from 3 to 39 $days$. These shorter events, highlighted by LFE bursts, were located downdip from L-SSEs (Frank et al., 2015b), at the transition from L-SSEs to the fully uncoupled interface. Using the LFE activity, the L-SSE of 2006 in Guerrero was shown to have an intermittent release of rapid pulses of tectonic stress during LFE episodes, and stress loading during inter-LFE periods (Frank et al., 2018).

To study the intermittence of aseismic slip in the Mexican subduction zone, we have post-processed GNSS time series using a trajectory model, following the method described in Marill et al. (2021). We then analyzed the TT catalog provided by Husker et al. (2019), covering a 10-year long period (2009 – 2018.5), to extract the periods of high TT activity, that we used to decompose GNSS time series into TT and inter-TT periods.

In the following work, we analyze separately the L-SSE periods (light blue spans in Fig. 2), during which we investigate the intermittence and variability of slow slip velocities, and the inter-L-SSE periods (white in Fig. 2) during which we search for S-SSEs. Since TT catalogs are given for single seismic stations (red triangles Fig. 1) and do not provide locations, the analysis is performed separately for Guerrero and Oaxaca regions (blue and green boxes in Fig. 1), considering for each region two tremors catalogs (from the seismic stations in red in Fig. 1).

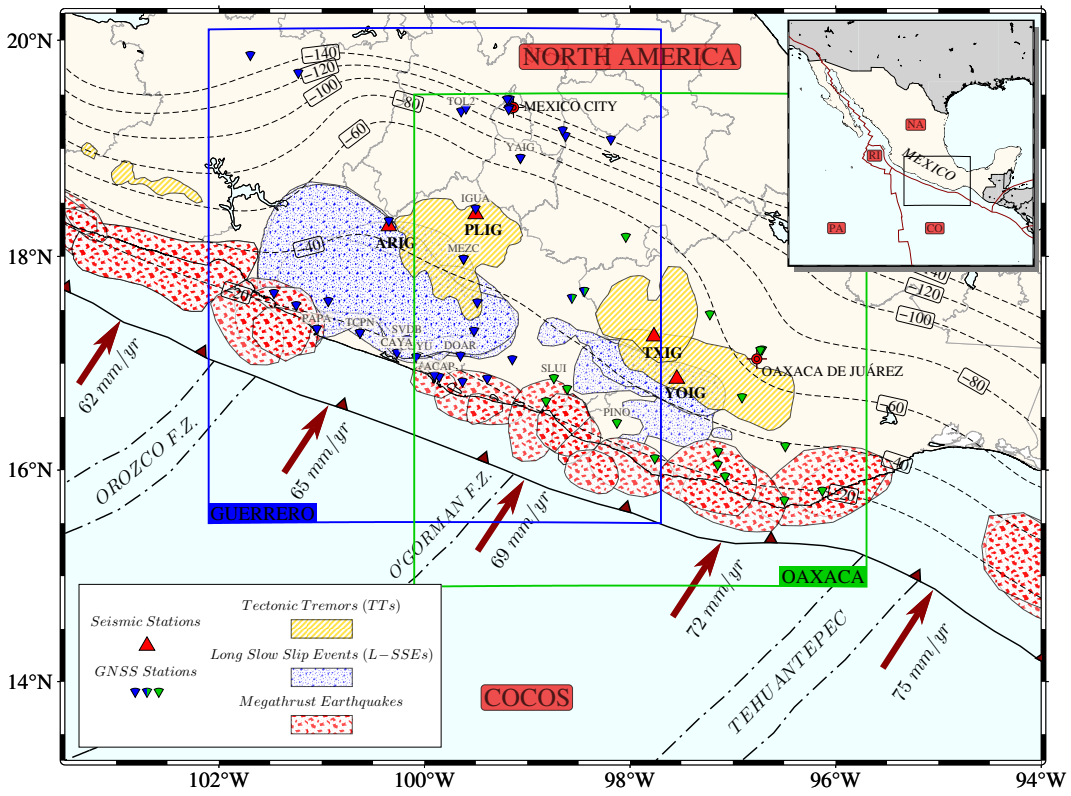

Figure 1: Tectonic context of the Mexican subduction zone. Historical earthquakes are shown by contours filled with red-colored patterns, L-SSEs are shown by contours filled with blue-colored patterns (Radiguet et al., 2011, 2016; Graham et al., 2016; Cruz-Atienza et al., 2021, from), and TTs are shown by contours filled with yellow-colored patterns (from Maury et al., 2018; Brudzinski et al., 2010; Ide, 2012). The red triangles are the seismic broad-band stations for which TT catalogs are used in this study (Husker et al., 2019), and the blue and green down-pointing triangles represent the GNSS stations used for the decomposition in Guerrero and Oaxaca respectively. The thin black dashed lines are the slab contours, Hayes et al. (2018). The blue rectangle delimits the study region of Guerrero, and the green rectangle delimits the study region of Oaxaca. The inset map shows the larger tectonic context with the tectonic plates (PA: Pacific plate, CO: Cocos plate, NA: North America plate, and RI: Rivera plate) (Bird, 2003).

2. Joint GNSS and Tectonic Tremor analysis

2.1. Seismic and Geodetic data

In this study, we have combined GNSS and TT data in order to analyze transient slow slips. We have used recordings from 33 GNSS sites in the Guerrero region, and 21 sites in the Oaxaca region (Respectively blue and green triangles in Fig. 1). The daily GNSS times series were processed with a double difference approach using the GAMIT/GLOBK software (Herring et al., 2010), the details of the processing can be found in the supplementary materials (1.1). We have also used 4 TT catalogs from Husker et al. (2019) for individual seismic stations, 2 of which are in the Guerrero region, and 2 in the Oaxaca region.

2.1.1. GNSS Trajectory Model and Common Modes

We fit the GNSS time series with a trajectory model, using the functional fitting method described in Marill et al. (2021). This model (Supplementary materials, eq. ES1) allows us to describe all the tectonic events observed in GNSS time series: inter-seismic periods with linear trends, earthquakes with Heaviside functions, post-seismic transients with decaying logarithmic functions, and L-SSEs with half-period cosine functions. We also modeled non-tectonic processes: seasonal variations with annual and semi-annual sines and cosines, and antenna jumps with Heaviside functions (Fig. 2.**B**). We then remove from the original GNSS time series the non-tectonic processes (seasonal and antenna jumps), as well as the linear interseismic trend, co-seismic and post-seismic offsets. The post-processed

GNSS time series (Fig. 2.**C**, and Fig. S2) thus still contain the L-SSE signals, as well as unmodeled signal and noise present in the residuals of the trajectory model. Note that although the L-SSEs function in the trajectory model is simple and does not reproduce all the displacement complexities, it allows to properly evaluate the other terms in the trajectory model. Since the modeled L-SSE terms are not removed from the original time series, this simple modeling is not influencing the rest of our analysis.

We then corrected the GNSS time series for common mode signals, which are low amplitude geodetic signals due to the mismodeling of satellite orbits and other large-scale phenomena common to the whole GNSS network. To extract the common modes, we followed the stacking method proposed by Márquez-Azúa and DeMets (2003). We choose 8 stations far from the study regions, at latitudes $> 20°N$, to ensure that the common modes do not contain tectonic signals. We computed the trajectory models of these 8 GNSS stations, and calculated the common mode by averaging the residual time series (Fig. S1). The average standard deviation on the northern component of the GNSS time series used in this study is ~ 1.55 *mm* and ~ 1.48 *mm* respectively before and after subtraction of common modes, which corresponds to a 5% reduction of the noise amplitude.

As a summary, the original GNSS time series (e.g. Fig. 2.**B**) are corrected from a trajectory model that includes a linear trend, co-seismic offsets, post-seismic relaxation, and annual and semi-annual oscillations, antenna-changes as well as common modes. The final time series (e.g. Fig. 2.**C** and S2) contain the residual noise and the L-SSE signals.

2.1.2. Tectonic Tremor Analysis

TTs are seismic signals emergent from the noise that can last up to several hours, with energy in the frequency band of 2 to 10 Hz. Husker et al. (2019) detected TTs for single seismic stations by analyzing the seismic spectral density in the TT frequency band. The TT catalogs provided by Husker et al. (2019) contain the starting and ending times of the detected high spectral energy periods (see Fig. S9 for an example of the catalog of tremor duration as a function of time), but no locations. Husker et al. (2019) derived four single station catalogs, two in the Guerrero region for the stations ARIG and PLIG, and two in the Oaxaca region for the stations TXIG and YOIG (Fig. 1).

In order to define the time periods when TT events are clustered, therefore when the rate of microseismicity is high, we computed the cumulative sum of TT durations over time, and corrected it from a linear trend (Fig. 2.**A**) to emphasize the temporal variations of TT activity. Positive slopes correspond to TT activity higher than average (tremor bursts) and negative slopes to activity lower than average (quiescence). High TT activity during documented L-SSEs is remarkable (e.g. L-SSEs of 2009, 2014, and 2017, light blue spans on Fig. 2.**A**). Shorter and less frequent bursts of high TT activity take over during inter-L-SSE periods (e.g. 2011-2014, grey spans Fig. 2.**A**). We have developed a simple method to systematically detect the start and end times of TT bursts from the detrended cumulated tremor durations (blue curve, Fig. 2.**A**). We compute the time derivative of this curve and keep only the positive values (i.e. positive slopes) as potential TT burst periods. We then firstly assembled TT bursts into a single burst if they are separated by a time period shorter than 3 *days*. Secondly, we discarded TT periods if their duration is lower than 3 *days*, and/or if the cumulated TT activity is lower than 10h. This method efficiently detects the majority of tremor bursts (i.e. positive slopes) visible on the detrended cumulated tremor activity time series (Fig. 2 and S8), while ensuring that the burst and inter-burst durations are not too short to be analyzed jointly with daily GNSS data (Fig. S9.**B**,**C**).

Using this method, we have independently detected TT bursts for the 4 TT catalogs (highlighted in grey in Fig. 2.**A** and Fig. S8.**A,B,D,E**). We identify tremor bursts ranging from 3 to 53 days, with average durations of 9 days and 13 days in Guerrero, for inter-L-SSEs and L-SSEs respectively, and average durations of 8 and 11 days in Oaxaca, for inter-L-SSEs and L-SSEs respectively (Fig. S10). As detailed in Fig. S8.**C,F**, the overlap between TT bursts for the two stations in the same region is important, 80% in Guerrero between ARIG and PLIG, and 75% in Oaxaca between TXIG and YOIG. This confirms that the tremors identified by a single station are well representative of a regional process. We selected the station PLIG to decompose for S-SSEs in the Guerrero region for its proximity to the sweet spot area. For L-SSEs, we choose the stations ARIG for its proximity to the transient zone in Guerrero, and the station TXIG in Oaxaca, because it has the best location with respect to the tremor zone localized by previous studies (yellow contours in Fig. 1).

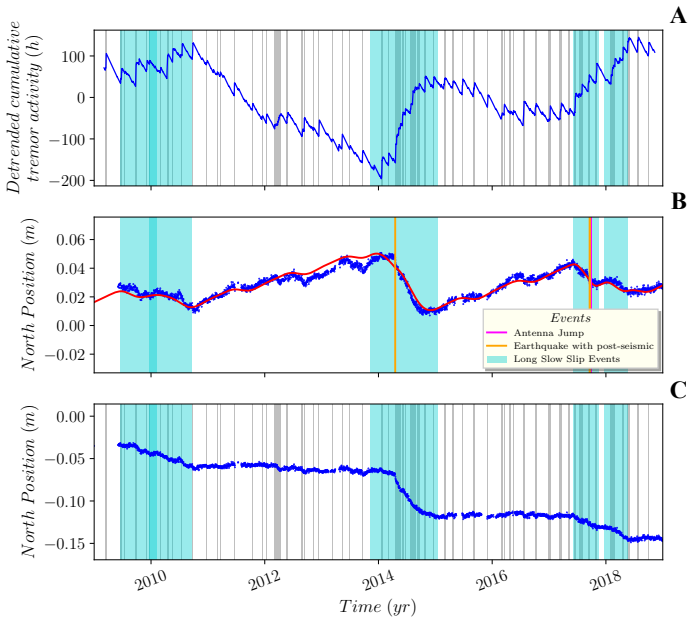

Figure 2: GNSS and tremor time series analysis. **A** TT burst detection for the seismic station PLIG. In blue, the detrended cumulative tremor durations. The grey lines show the detected TT bursts, and the light blue bands correspond to L-SSE periods, as determined using the L-SSE catalog in Table S2. **B** GNSS time series for the East component of the station IGUA. Blue points are the daily positions, and the trajectory model is in red. Vertical lines correspond to earthquakes with post-seismic relaxation in orange, and antenna jumps in magenta. **C** Residual (post-processed) time series including L-SSE signals (in blue). The grey spans are the detected TT bursts and the light blue bands show L-SSE periods.

2.2. *Data analysis*

2.2.1. *Decomposition of GNSS based on TT activity*

We combined the GNSS time series post-processed using a trajectory model and the detected TT bursts (blues dots and grey lines respectively in Fig. 2.**C**) to characterize transient slip intermittence during L-SSE and inter-L-SSE periods (respectively light blue and white period in Fig. 2). Previous studies showed that the amplitude of surface displacement for a single S-SSE in Guerrero is $\sim$ 1 *mm* (Frank et al., 2015b; Villafuerte and Cruz-Atienza, 2017), therefore it is below the noise level in GNSS time series. In order to extract such low amplitude signals, we decomposed GNSS time series based on the timing of TTs. For each tremor burst, we estimate the associated surface displacement offset, which corresponds to the difference in position between after and before the tremor burst. The positions before and after the bursts are estimated by averaging GNSS positions over a time window Δt which is equal to 6 days (see scheme Fig. S3.**A**). Because the positions are averaged over a time window Δt, the true duration of each tremor burst Δb (grey timespan in Fig. S3.**A**) is augmented by Δt (red timespan in Fig. S3.**A**) when computing the displacement rates associated with each tremor burst. In the same way, inter-TT true durations are reduced by Δt. The GNSS time series are then decomposed into TT and inter-TT periods by combining the calculated displacement offsets computed for each time period separately (grey and light red lines, Fig. 3.**A**,**B**).

Finally, we estimate the average velocity or displacement rate during TTs and inter-TTs using the total cumulative displacements and the cumulative durations (black and red arrows, Fig. 3.**A**,**B**). To account for data gaps in GNSS time series, we don't consider a TT and inter-TT period if more than 20% of GNSS data is missing in the considered time window. A range of averaging windows Δt between 2 to 16 days have been tested (Fig. S3.**B**). For short time windows, the final estimated displacement rates are strongly variable and sensitive to high frequency GNSS noise. Δt longer than 8 days under-estimated the displacement rates as the corrected tremor burst duration (red timespan in Fig. S3.**A**) increases. We thus select Δt = 6 days as the best compromise, with final estimated displacement rates being stable for all stations.

To test the reliability of our decompositions, we performed decompositions by shuffling in time the periods of TT bursts, while keeping the right TT burst durations, following the method described in Rousset et al. (2019b). The number of possible TT burst permutations for each tremor burst catalog can be calculated as $N!(N+1)!$, where N is the

number of tremor bursts. The decomposition at the station IGUA at inter-L-SSEs decomposes for 26 tremor bursts, giving $4.4 * 10^{54}$ possible permutations. For computational reasons and statistical representativeness, we consider 10^4 random permutation to calculate the uncertainty on the decompositions. The TT and inter-TT velocities resulting from the random decompositions are shown as histograms, for the north component of the stations IGUA (during inter-L-SSEs) and CAYA (during L-SSEs) in Fig. 3.**C**,**D**. The decomposition for TT bursts and inter-TT periods (bold black and red lines respectively) of a given GNSS station is considered reliable if the associated velocities are larger than the standard deviation of the distributions for decompositions with random TT burst times. In the following, at each GNSS station the standard deviations (σ in Fig. 3.**C**,**D**) calculated by decompositions with random TT burst times are used as uncertainties on the velocities for TT bursts and inter-TT periods. In addition to this analysis, after decomposing all GNSS time series, we kept only the results given by GNSS stations for which the completeness of the time series allowed to decompose for at least 5 TT bursts.

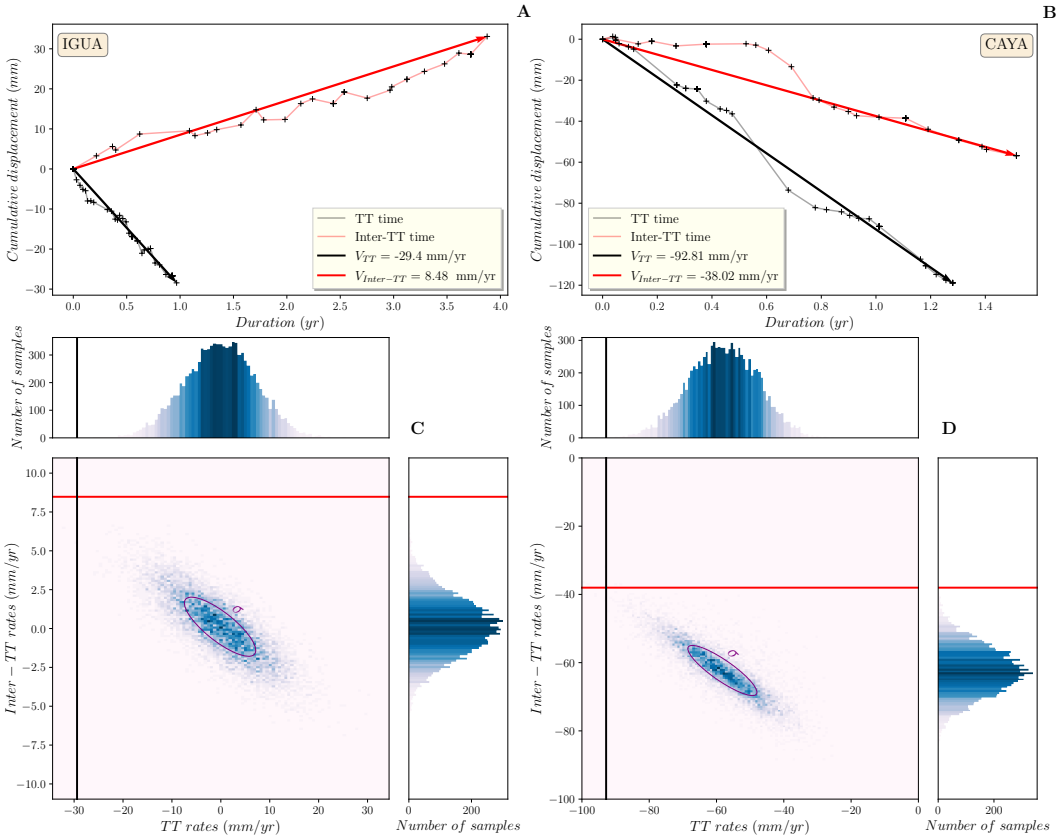

Figure 3: Examples of GNSS decompositions during inter-L-SSE periods (**A**) and L-SSE periods (**B**) and corresponding uncertainty estimation (**C**, **D**). **A** Decomposed cumulative displacements during inter-L-SSE periods for the North component of the GNSS site IGUA (Guerrero), based on the tremor catalog at the seismic site PLIG. The light black lines correspond to displacements during TT bursts and the light red lines correspond to displacements during inter-TT periods. Average velocities during TT bursts and inter-TT periods are shown by black and red bold arrows respectively. **B** Same as **A** but for L-SSE periods at the GNSS site CAYA (Guerrero), based on the tremor catalog at the site ARIG. **C** Decomposition velocities for the north component of the GNSS site IGUA with random times of the TT bursts, during inter-L-SSE periods. The top histogram show displacement rates calculated by decompositions with random TT burst times for TT periods, and the right histogram shows displacement rates for inter-TT periods. The central subplot is a 2D histogram made by combining the 2 lateral histograms, and purple ellipses show one standard deviation uncertainty (σ) of the Gaussian distribution. The black and red lines show TT and inter-TT velocities for the decomposition in (**A**), at the actual tremor times. **D** Same as **C**, but for L-SSEs decomposition at the GNSS site CAYA (**B**).

2.2.2. *Inversion of subduction interface slip rates*

Surface velocities calculated by decomposition of inter-L-SSE periods in GNSS time series (see 2.2.1), show trenchward motion (tectonic release) during TTs, and landward motion (tectonic loading) during inter-TT periods

Fig. 3.**A**,**B**. To characterize slip/backslip rates on the subduction interface associated with these surface motions, we performed a static linear least-squares inversion of surface velocities (see details in Supplementary materials 1.3). The 3D subduction interface from Slab 2.0 (Hayes et al., 2018), is discretized into triangular patches, and Green's functions are calculated for an elastic half-space using the formulation by Okada (1985). The slip direction is fixed according to the convergence direction ($\sim 28°N$). Regularization is selected as the best compromise between model roughness and data misfit. Poorly resolved areas, for which the restitution values (equation ES5) are low ($R_{rest} \leq 0.6$, see Fig. S7.**A**), are identified by yellow patch contours in the subduction plate locking maps. Plate locking in those areas is unresolved and close to zero, the a priori locking value assumed for the inversion. When studying S-SSEs, due to the lack of GNSS stations close to the seismic stations used for the decompositions, we gave in the inversion a weight 3 times higher to the few GNSS stations located inland, close to the seismic stations, as these stations showed the most reliable decomposition results.

3. Results

3.1. Long-term Slow Slip Events

We first looked at the detailed slip intermittence of the months-long SSEs (light blue spans in Fig. 2), previously observed and analyzed with GNSS data in several studies (e.g. Lowry et al., 2001; Kostoglodov, 2003; Radiguet et al., 2011; Graham et al., 2016; Cruz-Atienza et al., 2021). During L-SSEs, an important increase in TT activity is observed (Fig. 2.**A**,**B**). Our analysis of this activity (see 2.1.2) shows that TT bursts cover $\sim$ 30% of the duration of L-SSEs and up to 42% of the duration during the 2014 L-SSE in Guerrero (Fig. 2.**A**), with more energetic and longer lasting TT bursts than during inter-L-SSE periods. The decomposition of GNSS time series according to TT bursts was done using catalogs of the seismic stations ARIG and TXIG, for Guerrero and Oaxaca regions respectively. The results show that during TT bursts, surface displacement rates are towards the trench, corresponding to a release of accumulated strain. During inter-TT periods, the amplitude of surface velocities is lower, and shows a coherent spatial pattern as TT times.In Guerrero, slip rates during TTs are up to 0.24 m/yr (Fig. 4.**A**), and in Oaxaca up to 0.16 m/yr (Fig. 4.**C**). Slip rate contours during TTs correspond to areas where previous L-SSEs were located (e.g. L-SSE of 2010 in Guerrero, Radiguet et al. (2012), and L-SSE of 2016 in Oaxaca, Cruz-Atienza et al. (2021)). During inter-TT periods, the low amplitude slip rates are occurring at shallower depths (between 20 and 40 km). Both in Guerrero and Oaxaca, $\sim$ 65% of the total slip of L-SSEs occur within only 30% of their total duration, over TT periods ($\sum \Delta b$).

3.2. Short-term Slow Slip Events

Between L-SSEs, TT bursts provide a guide to detect S-SSE periods (Fig. 2.**C**). In order to characterize the associated aseismic slip amplitude, we decomposed the processed GNSS time series during these periods. The decomposition for TT periods, at the seismic stations PLIG and TXIG for the Guerrero and Oaxaca regions respectively, show surface displacement rates towards the trench, indicating transient release associated with S-SSEs (Fig. 5). During inter-TT times, the decompositions show landward surface displacement rates due to additional tectonic loading between S-SSEs. The average transient duration is 8 days in Oaxaca and 9 days in Guerrero (see histograms of durations in Fig. S10) and the average recurrence interval is 42 ± 11 days in Guerrero and 42 ± 13 days in Oaxaca, similar to the duration and recurrence times found using a geodetic matched filter, Rousset et al. (2017). On the most complete GNSS time series (IGUA), the results show the occurrence of 26 S-SSEs over the period 2009 - 2018.5, covering a cumulative duration of $\sim$ 0.6 *yr* of tremor activity. The maximum slip rates in the two study regions are co-located with TTs, with rates of $\sim$ 0.2 m/yr, close to the slip rates during TTs at L-SSE periods. In the Guerrero region, the high slip rate area corresponds to the S-SSE slip area found by Frank et al. (2015b), (Fig. 5.**A**), with maximum slip at a depth of 42 *km*. In the TTs transient zone in Guerrero, located immediately updip of the tremor patches, slip occurs both during S-SSEs and L-SSEs (Fig. 4.**A** and Fig. 5.**A**). In the Oaxaca region, we show for the first time the presence of S-SSEs, co-located with the tremor location and with maximum slip rates at the depth of 45 *km*, similar to Guerrero.

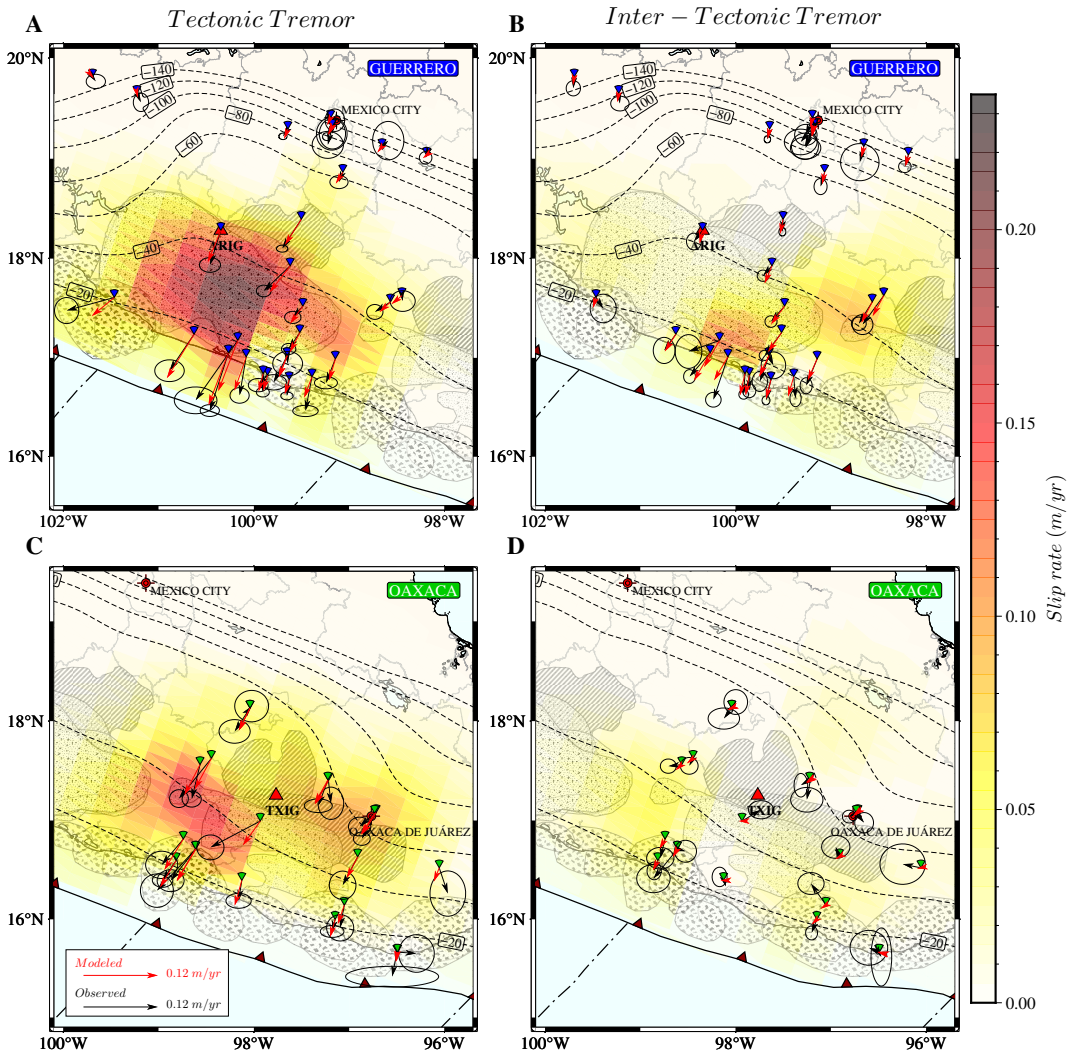

Figure 4: Maps of surface displacement rates and inferred slip rates for L-SSE periods, during TT bursts (left column) and inter-TT periods (right column). The results are presented for the Guerrero region on the top row and the Oaxaca region on the bottom row. The black arrows correspond to decomposed surface displacement rates topped with 1σ uncertainty ellipses. The red arrows correspond to the modeled prediction from the inverted slip rates shown by the colormap.

3.3. Subduction interface locking

In the Mexican subduction zone, the accumulated elastic strain of the overhanging plate can be released by large earthquakes or aseismic transient slips such as L-SSEs or S-SSEs. Here we analyze how loading occurs during inter-L-SSE and inter-S-SSE periods, by looking at the degree of locking at the subduction interface. We consider the MORVEL 2010 model as a reference for long-term convergence velocity in the region (DeMets et al., 2010). We extracted inter-L-SSE loading velocities from the trajectory models of GNSS time series (see 2.1.1) (Fig. S7.**B**), and we also extracted the increase of loading during inter-S-SSE periods from the GNSS decompositions (see 2.2.1). In order to obtain the complete loading velocities in inter-S-SSE periods, we summed the contribution of these two loading velocities. The inter-S-SSE locking derived from the summed velocities (Fig. 6.**A**) presents locking degrees above 0.7 in most areas of the resolved subduction interface. The locking pattern is similar to the ones obtained in previous studies (Radiguet et al., 2012; Rousset et al., 2016; Maubant et al., 2022) but with increased locking at S-SSEs locations. In order to highlight the increase of locking in between S-SSEs, we also looked at the difference between the inter-L-SSEs and inter-S-SSEs locking models (Fig. 6.**B**). It shows an increase of locking up to 0.5,

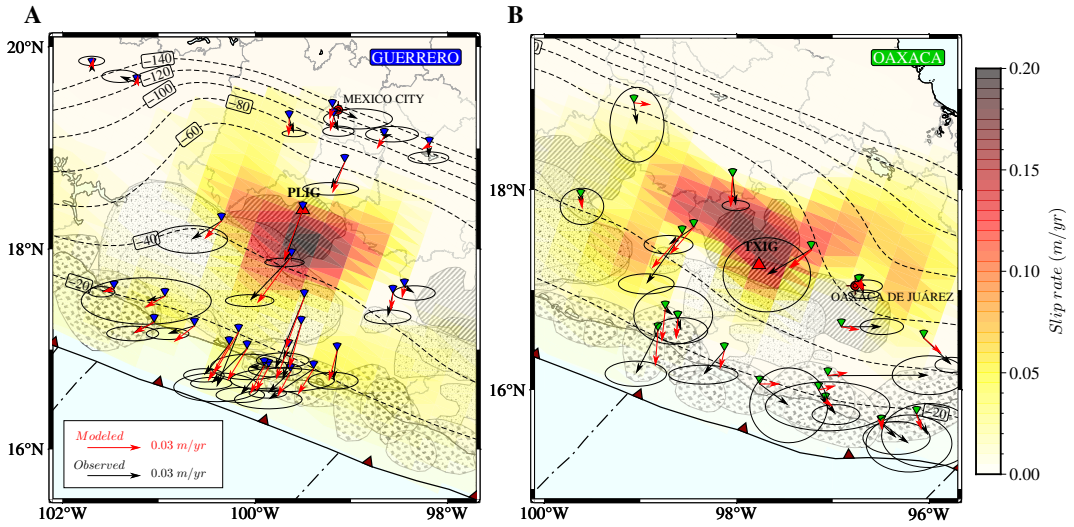

Figure 5: Maps of surface displacement rates and inferred slip rates for S-SSEs associated with TT bursts during inter-L-SSE periods. **A** Results for the Guerrero region. The black arrows correspond to decomposed surface displacement rates during TT bursts, topped with 1σ uncertainty ellipses. The red arrows correspond to the model predictions from the inverted slip rates shown by the colormap. **B** Same as **A** but for the Oaxaca region.

compatible with S-SSE locations (Fig. 5). This observation reveals that at short time scales, the plate interface has a high locking ratio at depths down to 50 km, far below the previously observed downdip limit of the seismogenic zone.

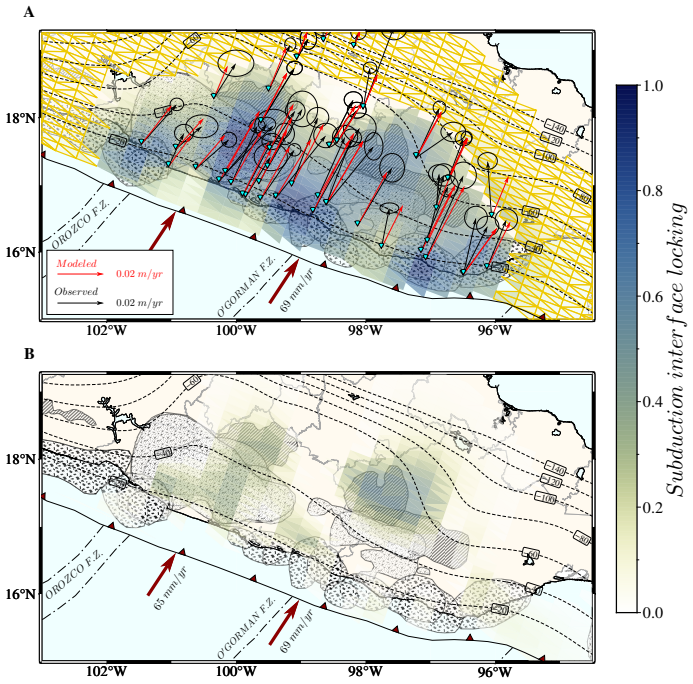

Figure 6: Locking maps for inter-S-SSE time periods (**A**) and additional short time scale locking estimated in this study (**B**). **A** Inter-S-SSE loading velocities are the black arrows, with 1σ uncertainty ellipses. The red arrows show the prediction from the locking model displayed with the colormap. The yellow triangles indicate areas poorly resolved, with a restitution index $R_{rest} \leq 0.6$. **B** Map of the difference between inter-S-SSE locking in **A** and the first order inter-L-SSEs locking (Fig. S7.**B**) estimates. Note that high locking areas during inter-S-SSEs correspond to high slip rate areas during S-SSEs (Fig. 5).

4. Discussion

4.1. Characterisation of slip bursts in Guerrero and Oaxaca regions

Our study shows that transient aseismic slip on the Mexican subduction zone is characterized by short-lasting slip bursts with durations from 3 to 53 days. Two distinct behaviors and slip locations are observed. The first one is associated with L-SSEs, which are made of clusters of slip accelerations. We observe two distinct slip regions located just below the seismogenic zone in Guerrero and Oaxaca regions (Fig. 8). The second behavior occurs in inter-L-SSE periods, during which S-SSEs are observed at the down-dip end of the transient slip area, co-located with tectonic tremors. We identified two distinct areas of S-SSEs, in Guerrero and Oaxaca, located at the downdip edges of L-SSEs in both regions.

The average S-SSEs location in Guerrero is compatible with previous studies (Frank et al., 2015b; Villafuerte and Cruz-Atienza, 2017). Our analysis during the period 2009 - 2018.5 characterizes S-SSEs with an average duration of 9 days, 1 day longer than previous studies, and 42 ± 11 days recurrence intervals, shorter than the 3 months recurrence observed by Frank et al. (2015b). This difference could be due to the different time periods considered, or due to the different micro-seismic markers used for the decomposition of GNSS time series. In the Oaxaca region, our results unveil the presence of S-SSEs, with an average duration of 8 days and average recurrence intervals of 42 ± 13 days, similar to the observed results in the Guerrero region. Interestingly, the S-SSE region in Oaxaca that we identified, encompasses an area (longitudes between -98° and -99°) where some small SSE detections were made using a geodetic matched filter analysis by Rousset et al. (2017), but also extends further East. We thus infer that these events previously identified with geodetic template matching over a different time period (2005-2012), probably also correspond to S-SSE in Oaxaca, even if their correlation with tremor activity has not been demonstrated.

The distinction of L-SSEs in the Guerrero and Oaxaca regions has been made in previous studies, showing an alternation of slip between the two regions (Graham et al., 2014, 2016; Cruz-Atienza et al., 2021). While in Guerrero, L-SSEs have larger magnitudes than in Oaxaca, we show that S-SSEs in Guerrero and Oaxaca have similar average slip rates and rupture areas (Table S1). By looking at the temporal overlap of TT catalogs for the two regions, we show that the two catalogs overlap only 12% of the time (Fig. S8.**G,H,I**), suggesting that S-SSEs occur independently in the two regions. No slip interaction between the two regions could be observed by our study, emphasizing previous studies looking at Coulomb stress changes (Graham et al., 2014).

4.2. Limitations of single station tremor catalogs

One limitation of our analysis is that the tremor catalogs that we use are obtained for individual single seismic stations and do not provide events location. Consequently, such catalogs are not necessarily complete and depend on the location of the seismic stations with respect to the tremor sources. This raises the question of the representativeness of a mono-station catalog to characterize the regional tremor activity. The comparison between the two catalogs available in Guerrero (ARIG and PLIG) shows 80% overlap in the tremor burst detection (Fig. S8.**A,B,C**). It shows that although the station ARIG is closer to the coast and likely less sensitive to deep tremors occurring in the sweet spot than PLIG, both stations capture similar features corresponding to the regional tremor activity. The same is true in Oaxaca with TXIG and YOIG catalogs showing 75% overlap (Fig. S8.**D,E,F**). Using one seismic station or another to characterize the tremor bursts within a given region thus leads to similar decomposition results. Complete tremor catalogs with proper locations should potentially allow to discriminate slip located on the sweet spot and the transient zone by doing separate GNSS decompositions for the two tremor locations.

4.3. Deep and shallow slip in Guerrero during S-SSEs

During S-SSEs in the Guerrero region, slip rates of low amplitude are noticeable offshore, in the Guerrero seismic gap (Fig. 5.**A**). This shallow slip is suggested by GNSS stations close to the coast that has trenchward S-SSE velocities higher than the estimated uncertainties. We have tested an inverse model without shallow slip, by penalizing slip rates at depths lower than 35 km (Fig. S5). Such models present a single slip patch at the TTs location, but the important misfit at coastal GNSS sites suggests that shallow slip is required to explain the data. A similar aseismic slip configuration with simultaneous slip below and above the seismogenic zone has also been observed in the Nankai Trough by Kano et al. (2015), and explained by possible up-dip fluid migration that percolated through the seismogenic zone. In the Mexico subduction zone, offshore tremors and repeating earthquake swarms were unveiled and characterized with ocean bottom seismometers (Plata-Martinez et al., 2021). These shallow events show a correlation in some cases with deep TT (Fig. S14), suggesting a large-scale phenomenon, and possible deep-shallow tremor interactions.

4.4. *Dynamics of long-term transients and comparison with previous works*

We show that L-SSEs are made of clusters of slip accelerations that happen at the times of TT bursts, both in Guerrero and Oaxaca. This observation is possible only by combining information from tremor timings and GNSS positioning. Previous GNSS only studies (Lowry et al., 2001; Radiguet et al., 2011; Graham et al., 2016; Cruz-Atienza et al., 2021), could not reveal these short-term slip accelerations. In the Alaska subduction zone, a similar observation of slip acceleration associated with tremor bursts was made for a 5 years-long slow slip event, and revealed that $\sim$ 80% of the M_w 7.2 event's moment had been released during TT bursts (Rousset et al., 2019b).

The clustering of the Guerrero L-SSEs into shorter events has been observed for the 2006 event by Frank et al. (2018), who decomposed GNSS time series based on LFEs activity. Our analysis gives similar results qualitatively. In both studies, about 30% of L-SSE correspond to bursts of seismic activity (tremors or LFEs), during which surface velocities are higher than the average SSE surface velocity (see Fig.7 and Fig. S11 for examples of surface velocity decompositions from L-SSEs after 2009 and the L-SSE of 2006 Frank et al. (2018) respectively).

To compare in more detail the decomposition method used in this study and the results from Frank et al. (2018), we decomposed the GNSS time series during the 2006 L-SSE with our burst detection method, applied to the LFE catalog (Fig. S11). We used the LFE catalog that contains only the events of the transient zone (Frank et al., 2018) (Fig. S11.**A**), with average tremor burst durations of 17 days. The displacement rates obtained by our decomposition method show slightly higher rates during LFE periods than inter-LFEs (Fig. S11.**C**-**F**). However, the velocities obtained by Frank et al. (2018) decomposition's method are 2 to 3 times higher than the ones obtained with our method. The decompositions obtained with our method for the whole LFE catalog (Frank et al., 2014) (Fig. S11.**B**, including the transient zone and the sweet spot) with an average LFE burst duration of 6 days and including more LFE bursts than the transient zone alone, also show decompositions with higher rates during LFE periods (Fig. S11.**G**-**J**). Given that the study period of the 2006 SSE is short and the number of LFE bursts is limited, the decomposition results are less reliable than for the stacked decomposition of SSEs over a 10 years period which include more than one year of cumulated displacement and more than 25 tremor bursts.

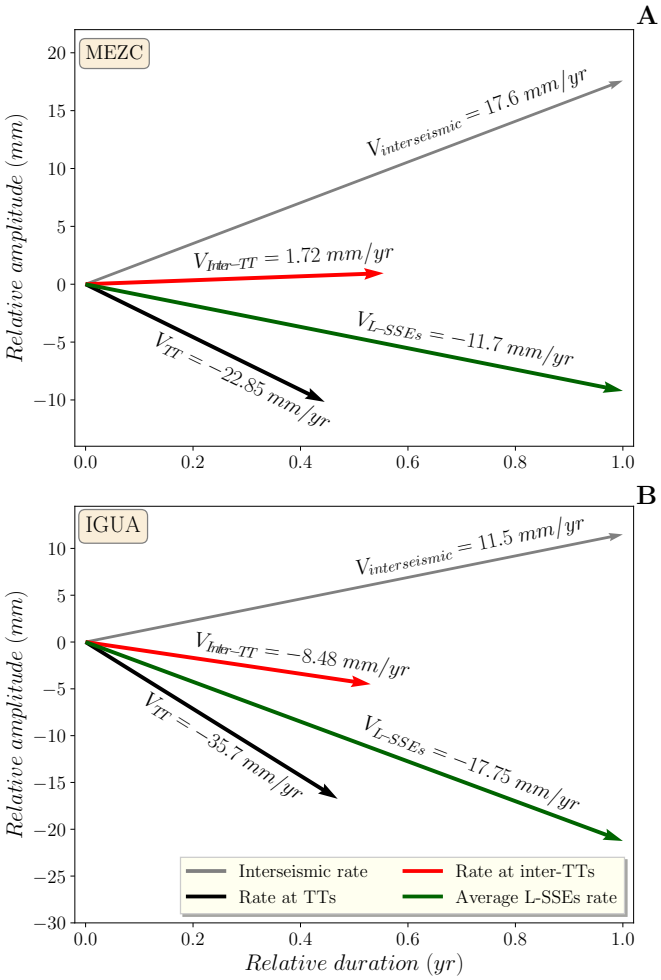

Figure 7: Decomposition of GNSS time series for L-SSEs using the TT bursts at the GNSS stations MEZC and IGUA (**A** and **B** respectively). The black arrows are surface rates during TT periods. The red arrows are the surface velocities for inter-TT periods. The dark green arrows are the sum of the black and the red arrows, and correspond to the mean surface velocity during L-SSE. The grey arrows are the interseismic velocities calculated using a trajectory model. Note that the durations have been normalized along the x-axis to facilitate the comparison between the rates

4.5. Slip initiation and propagation rates

The largest slip amplitudes during L-SSEs are located updip from the TT area, while slip and TTs are happening simultaneously as shown by our decomposition results (Fig. 4). The elastic updip stress built-up during inter-L-SSEs by successive S-SSEs might explain the along dip succession of S-SSEs and L-SSEs over time (Wech and Creager, 2011). It is also possible that pore fluid pressure increases during the inter-L-SSEs, updip of S-SSEs, facilitating the initiation and propagation of slip during L-SSEs throughout an area wider than the TT zone (Frank et al., 2015b; Kano et al., 2015). In Guerrero, TT locations corresponds to dehydration depths, where metamorphism occurs (Manea et al., 2004). Updip from this location, a fluid saturated ultra-slow velocity layer (USL) was observed from seismic recordings (Song et al., 2009). A possible explanation for the permanent high pore pressure in this area is the trapped fluids in the fault zone due to an impermeable gabbroic layer in the lower crust of the North America plate (Husker et al., 2017). Variations in fluid pore pressure modulated by a deeper source could be the triggering factor of slip intermittence at USL depths during L-SSEs.

Our observational results provide some constrains on the average slip rates and propagation velocity of the slip burst during TT periods. S-SSE slip episodes last on average 9 days (Fig. S9), and have average slip rates of 0.2

m/yr (Fig. 8). Considering that the slow slip front initiated in the deeper part of the tremor zone and migrated updid over an along-dip distance of 80-90km, this leads to an updip migration velocity of around 10 km/day. We have limited constrain on the along-strike migration velocity as the lateral extent of the S-SSE zone is poorly constrained. Considering a S-SSE width of 110km, and a rupture that can propagate unilaterally or bilaterally, we can estimate an along-strike propagation velocity in the range of $6 - 12$ km/day, which is consistent with estimates for SSEs in the Cascadia and Alaska subduction zones (Wech et al., 2009; Rousset et al., 2019b).

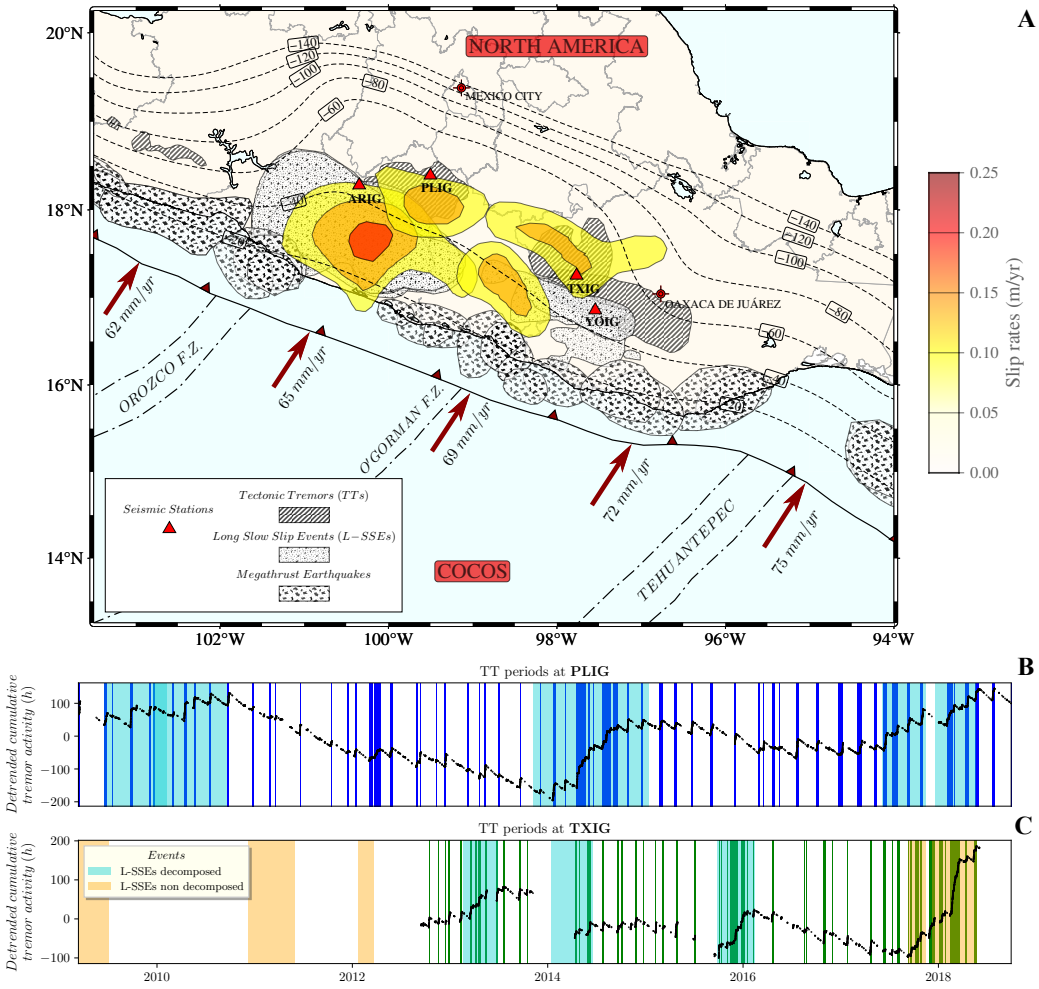

Figure 8: Slip rate of S-SSEs and L-SSEs in the Guerrero and Oaxaca regions. The map (**A**) shows the slip rate contours for S-SSEs, which are colocated with the tremor areas, and the updip slip rate contours for L-SSEs. All the black contours with patterns are the same as in Fig. 1. Figure **B** shows the cumulated and detrended tremor activity time series as black dots, at the seismic station PLIG. The tremor burst periods, as dark blue spans. L-SSE periods in the Guerrero region are shown as light blue spans. Figure **C** shows the cumulated and detrended tremor activity time series as black dots, at the seismic station TXIG. The tremor burst periods, as green spans. L-SSE periods in the Oaxaca region are shown as light blue spans if they are used in the decompositions, or as yellow spans if they are not decomposed.

5. Conclusions

We analyzed jointly tectonic tremors and GNSS observations on the Guerrero and Oaxaca regions of the Mexican subduction zone. GNSS time series are decomposed relative to tremor times, to obtain average slip rates associated with tectonic tremors. During large slow slip events (L-SSEs), slip rates are not constant in time but accelerate during tectonic tremor bursts, and the largest slip rates are located updip from the tectonic tremors location. This observation

is made for large SSEs in both for Guerrero and Oaxaca regions, although their total moment magnitudes are different. In between large transient slip events, smaller transient slip events (S-SSEs) are also observed, correlated in time and space with tectonic tremors. While these short-term slip events were already documented in Guerrero, our study unveil short-term slip events in Oaxaca for the first time. In Guerrero, short-term slip events have average magnitudes M_w of 6.6, average duration of 9 days and recurrence intervals of 42 ± 11 days, while in Oaxaca, they have average M_w of 6.5, average duration of 8 days, and recurrence intervals of 42 ± 13 days. Tectonic tremor timings show that transient slips are alternating between the Guerrero and Oaxaca regions, both for long-term and short-term transient slip events. The analysis of tectonic loading periods, at short time scale between short-term transients, shows that the inter-plate locking increases by up to 0.5 at tectonic tremor depths compared to what was identified by previous studies. This confirms that the plate interface locking varies at short temporal scales.

Acknowledgments

We thank people who maintain the cGPS networks in Guerrero (IG-UNAM) and Oaxaca (TLALOCNet program) states, in particular J. A. Santiago at the Servicio Mareografico Nacional-UNAM, S. I. Franco at the Servicio Sismologico Nacional-UNAM. This study has been supported by the Agence Nationale de la Recherche (ANR-21-CE49-0023) SSDYN project, and by the Universidad Nacional Autónoma de México PAPIIT-IG100921 project. We also thank William Frank for discussion and comparison with his work, and Yuji Itoh for discussion about GNSS time series decomposition.

References

Bartlow, N.M., 2020. A long-term view of episodic tremor and slip in cascadia. Geophysical Research Letters 47, e2019GL085303. doi:10.1029/2019GL085303.

Beroza, G.C., Ide, S., 2011. Slow earthquakes and nonvolcanic tremor. Annual Review of Earth and Planetary Sciences 39, 271–296. doi:10.1146/annurev-earth-040809-152531.

Bird, P., 2003. An updated digital model of plate boundaries. Geochemistry, Geophysics, Geosystems 4(3), 1027. doi:10.1029/2001GC000252.

Brudzinski, M.R., Hinojosa-Prieto, H.R., Schlanser, K.M., Cabral-Cano, E., Arciniega-Ceballos, A., Diaz-Molina, O., DeMets, C., 2010. Nonvolcanic tremor along the oaxaca segment of the middle america subduction zone. Journal of Geophysical Research: Solid Earth 115. doi:10.1029/2008JB006061.

Cruz-Atienza, V.M., Husker, A., Legrand, D., Caballero, E., Kostoglodov, V., 2015. Nonvolcanic tremor locations and mechanisms in guerrero, mexico, from energy-based and particle motion polarization analysis. Journal of Geophysical Research: Solid Earth 120, 275–289. doi:10.1002/2014JB011389.

Cruz-Atienza, V.M., Tago, J., Villafuerte, C., Wei, M., Garza-Girón, R., Dominguez, L.A., Kostoglodov, V., Nishimura, T., Franco, S.I., Real, J., Santoyo, M.A., Ito, Y., Kazachkina, E., 2021. Short-term interaction between silent and devastating earthquakes in mexico. Nature Communications 12(1), 2172. doi:10.1038/s41467-021-22326-6.

DeMets, C., Gordon, R.G., Argus, D.F., 2010. Geologically current plate motions. Geophysical Journal International 181, 1–80. doi:10.1111/j.1365-246X.2009.04491.x.

Dragert, H., 2001. A silent slip event on the deeper cascadia subduction interface. Science 292(5521), 1525–1528. doi:10.1126/science.1060152.

Frank, W., Rousset, B., Lasserre, C., Campillo, M., 2018. Revealing the cluster of slow transients behind a large slow slip event. Science Advances 4, eaat0661. doi:10.1126/sciadv.aat0661.

Frank, W., Shapiro, N., Husker, A., Kostoglodov, V., Bhat, H., Campillo, M., 2015a. Along-fault pore-pressure evolution during a slow-slip event in guerrero, mexico. Earth and Planetary Science Letters 413, 135–143. doi:10.1016/j.epsl.2014.12.051.

Frank, W.B., 2016. Slow slip hidden in the noise: The intermittence of tectonic release. Geophysical Research Letters 43, 10,125–10,133. doi:10.1002/2016GL069537.

Frank, W.B., Radiguet, M., Rousset, B., Shapiro, N.M., Husker, A.L., Kostoglodov, V., Cotte, N., Campillo, M., 2015b. Uncovering the geodetic signature of silent slip through repeating earthquakes. Geophysical Reasearch Letters 42, 2774– 2779. doi:10.1002/2015GL063685.

Frank, W.B., Shapiro, N.M., 2014. Automatic detection of low-frequency earthquakes (lfes) based on a beamformed network response. Geophysical Journal International 197, 1215–1223. doi:10.1093/gji/ggu058.

Frank, W.B., Shapiro, N.M., Husker, A.L., Kostoglodov, V., Romanenko, A., Campillo, M., 2014. Using systematically characterized low-frequency earthquakes as a fault probe in guerrero, mexico. Journal of Geophysical Research: Solid Earth 119, 7686–7700. doi:10.1002/2014JB011457.

Fu, Y., Freymueller, J.T., 2013. Repeated large slow slip events at the southcentral alaska subduction zone. Earth and Planetary Science Letters 375, 303–211. doi:10.1016/j.epsl.2013.05.049.

Fujita, M., Nishimura, T., Miyazaki, S., 2019. Detection of small crustal deformation caused by slow slip events in southwest japan using gnss and tremor data. Earth, Planets and Space 71(96). doi:10.1186/s40623-019-1075-x.

Graham, S., DeMets, C., Cabral-Cano, E., Kostoglodov, V., Rousset, B., Walpersdorf, A., Cotte, N., Lasserre, C., McCaffrey, R., Salazar-Tlaczani, L., 2016. Slow slip history for the mexico subduction zone: 2005 through 2011. Pure and Applied Geophysics 173, 3445–3465. doi:10.1007/s00024-015-1211-x.

Graham, S.E., DeMets, C., Cabral-Cano, E., Kostoglodov, V., Walpersdorf, A., Cotte, N., Brudzinski, M., McCaffrey, R., Salazar-Tlaczani, L., 2014. Gps constraints on the 2011-2012 oaxaca slow slip event that preceded the 2012 march 20 ometepec earthquake, southern mexico. Geophysical Journal International 197(3), 1593–1607. doi:10.1093/gji/ggu019.

Hayes, G.P., Moore, G.L., Portner, D.E., Hearne, M., Flamme, H., Furtney, M., Smoczyk, G.M., 2018. Slab2, a comprehensive subduction zone geometry model. Science 362, 58–61. doi:10.1126/science.aat4723.

Herring, T.A., King, R.W., McClusky, S.C., 2010. Introduction to gamit/globk. Massachusetts Institute of Technology, Cambridge, Massachusetts .

Hirose, H., Hirahara, K., Kimata, F., Fuji, N., Miyazaki, S., 1999. A slow thrust slip event following the two 1996 hyuganada earthquakes beneath the bungo channel, southwest japan. Geophysical Research Letters 26(21), 3237–3240. doi:10.1029/1999gl010999.

Husker, A., Ferrari, L., Arango-Galván, C., Corbo-Camargo, F., Arzate-Flores, J.A., 2017. A geologic recipe for transient slip within the seismogenic zone: Insight from the Guerrero seismic gap, Mexico. Geology 46, 35–38. doi:10.1130/G39202.1.

Husker, A., Frank, W.B., Gonzalez, G., Avila, L., Kostoglodov, V., Kazachkina, E., 2019. Characteristic tectonic tremor activity observed over multiple slow slip cycles in the mexican subduction zone. Journal of Geophysical Research: Solid Earth 124, 599–608. doi:10.1029/2018JB016517.

Husker, A.L., Kostoglodov, V., Cruz-Atienza, V.M., Legrand, D., Shapiro, N.M., Payero, J.S., Campillo, M., Huesca-Pérez, E., 2012. Temporal variations of non-volcanic tremor (nvt) locations in the mexican subduction zone: Finding the nvt sweet spot. Geochemistry, Geophysics, Geosystems 13. doi:10.1029/2011GC003916.

Ide, S., 2012. Variety and spatial heterogeneity of tectonic tremor worldwide. Journal of Geophysical Research: Solid Earth 117. doi:10.1029/2011JB008840.

Kano, M., Kato, A., Obara, K., 2015. Episodic tremor and slip silently invades strongly locked megathrust in the nankai trough. Science 9, 9270. doi:10.1038/s41598-019-45781-0.

Kostoglodov, V., 2003. A large silent earthquake in the guerrero seismic gap, mexico. Geophysical Research Letters 30(15), 1807. doi:10.1029/2003gl017219.

Lowry, A.R., Larson, K.M., Kostoglodov, V., Bilham, R., 2001. Transient fault slip in guerrero, southern mexico. Geophysical Research Letters 28(19), 3753–3756. doi:10.1029/2001gl013238.

Manea, V., Manea, M., Ferrari, L., Orozco-Esquivel, T., Valenzuela, R., Husker, A., Kostoglodov, V., 2017. A review of the geodynamic evolution of flat slab subduction in mexico, peru, and chile. Tectonophysics 695, 27–52. doi:10.1016/j.tecto.2016.11.037.

Manea, V.C., Manea, M., Kostoglodov, V., Currie, C.A., Sewell, G., 2004. Thermal structure, coupling and metamorphism in the Mexican subduction zone beneath Guerrero. Geophysical Journal International 158, 775–784. doi:10.1111/j.1365-246X.2004.02325.x.

Marill, L., Marsan, D., Socquet, A., Radiguet, M., Cotte, N., Rousset, B., 2021. 14-year acceleration along the japan trench and the sagami trough. Earth and Space Science Open Archive doi:10.1002/essoar.10504635.1.

Maubant, L., Radiguet, M., Pathier, E., Doin, M.P., Cotte, N., Kazachkina, E., Kostoglodov, V., 2022. Interseismic coupling along the mexican subduction zone seen by insar and gnss. Earth and Planetary Science Letters 586, 117534. doi:10.1016/j.epsl.2022.117534.

Maury, J., Ide, S., Cruz-Atienza, V.M., Kostoglodov, V., 2018. Spatiotemporal variations in slow earthquakes along the mexican subduction zone. Journal of Geophysical Research: Solid Earth 123, 1559–1575. doi:10.1002/2017JB014690.

Márquez-Azúa, B., DeMets, C., 2003. Crustal velocity field of mexico from continuous gps measurements, 1993 to june 2001: Implications for the neotectonics of mexico. Journal of Geophysical Research 108(B9), 2450. doi:10.1029/2002jb002241.

Obara, K., 2002. Nonvolcanic deep tremor associated with subduction in southwest japan. Science 296, 1679–1681. doi:10.1126/science.1070378.

Okada, Y., 1985. Surface deformation due to shear and tensile faults in a half-space. Bulletin of the Seismological Society of America 1985 75(4), 1135–1154. doi:10.1785/BSSA0750041135.

Payero, J.S., Kostoglodov, V., Shapiro, N., Mikumo, T., Iglesias, A., Pérez-Campos, X., Clayton, R.W., 2008. Nonvolcanic tremor observed in the mexican subduction zone. Geophysical Research Letters 35. doi:10.1029/2007GL032877.

Plata-Martinez, R., Ide, S., Shinohara, M., Garcia, E.S., Mizuno, N., Dominguez, L.A., Taira, T., Yamashita, Y., Toh, A., Yamada, T., Real, J., Husker, A., Cruz-Atienza, V.M., Ito, Y., 2021. Shallow slow earthquakes to decipher future catastrophic earthquakes in the guerrero seismic gap. Nature Communications 12, 3976. doi:10.1038/s41467-021-24210-9.

Radiguet, M., Cotton, F., Vergnolle, M., Campillo, M., Valette, B., Kostoglodov, V., Cotte, N., 2011. Spatial and temporal evolution of a long term slow slip event: the 2006 guerrero slow slip event. Journal of Geophysical Research: Solid Earth 184(2), 816–828. doi:10.1111/j.1365-246x.2010.04866.x.

Radiguet, M., Cotton, F., Vergnolle, M., Campillo, M., Walpersdorf, A., Cotte, N., Kostoglodov, V., 2012. Slow slip events and strain accumulation in the guerrero gap, mexico. Journal of Geophysical Research 117(B4). doi:10.1029/2011jb008801.

Radiguet, M., Perfettini, H., Cotte, N., Gualandi, A., Valette, B., Kostoglodov, V., Lhomme, T., Walpersdorf, A., Cabral Cano, E., Campillo, M., 2016. Triggering of the 2014 mw7.3 papanoa earthquake by a slow slip event in guerrero, mexico. Nature Geoscience 9, 829–833. doi:10.1038/ngeo2817.

Rousset, B., Bürgmann, R., Campillo, M., 2019a. Slow slip events in the roots of the san andreas fault. Science Advances 5(2), eaav3274. doi:10.1126/sciadv.aav3274.

Rousset, B., Campillo, M., Lasserre, C., Frank, W.B., Cotte, N., Walpersdorf, A., Socquet, A., Kostoglodov, V., 2017. A geodetic matched-filter search for slow slip with application to the mexico subduction zone. Journal of Geophysical Research: Solid Earth 122, 10,498– 10,514. doi:10.1002/2017JB014448.

Rousset, B., Fu, Y., Bartlow, N.M., Bürgmann, R., 2019b. Weeks-long and years-long slow slip and tectonic tremor episodes on the south central alaska megathrust. Journal of Geophysical Research: Solid Earth 124, 13392–13403. doi:10.1029/2019JB018724.

Rousset, B., Lasserre, C., Cubas, N., Graham, S., Radiguet, M., DeMets, C., Socquet, A., Campillo, M., Kostoglodov, V., Cabral-Cano, E., Cotte, N., Walpersdorf, A., 2016. Lateral variations of interplate coupling along the mexican subduction interface: Relationships with long-term morphology and fault zone mechanical properties. Pure and Applied Geophysics 173(10), 3467–3486. doi:10.1007/s00024-015-1215-6.

Song, T.R.A., Helmberger, D.V., Brudzinski, M.R., Clayton, R.W., Davis, P., Perez-Campos, X., Singh, S.K., 2009. Subducting slab ultra-slow velocity layer coincident with silent earthquakes in southern mexico. Science 324(5926), 502–506. doi:10.1126/science.1167595.

Villafuerte, C., Cruz-Atienza, V.M., 2017. Insights into the causal relationship between slow slip and tectonic tremor in guerrero, mexico. Journal

of Geophysical Research: Solid Earth 122, 6642–6656. doi:10.1002/2017JB014037.
Wech, A.G., Creager, K.C., 2011. A continuum of stress, strength and slip in the cascadia subduction zone. Nature Geoscience 4, 624–628. doi:10.1038/ngeo1215.
Wech, A.G., Creager, K.C., Melbourne, T.I., 2009. Seismic and geodetic constraints on cascadia slow slip. Journal of Geophysical Research: Solid Earth 114. doi:10.1029/2008JB006090.

